energies

Article

# Comparison Study on High Force Density Linear Motors for Compressor Application

**Fei Zhao [1,*], Yunshuai Jiang [1], Kuang Yang [1], Chengming Zhang [2], Wei Lian [3] and Guangyin Wang [4]**

[1] Power Electronics and Electrical Drives Center, Harbin Institute of Technology (Shenzhen), Shenzhen 518055, China; 20S153258@stu.hit.edu.cn (Y.J.); yangkuang@stu.hit.edu.cn (K.Y.)
[2] Department of Electrical Engineering, Harbin Institute of Technology, Harbin 150006, China; cmzhang@hit.edu.cn
[3] Ming Lianxing Mechanical Technology Co., Ltd., Wenzhou 325000, China; 13316880177@163.com
[4] Office of Military Representative Bureau, Beijing 100000, China; gyin_w@aliyun.com
* Correspondence: fzhao@hit.edu.cn

**Abstract:** This paper presents the modular topologies of the dual-stator dual-winding permanent magnet (PM) linear motors for linear compressors used in the electrified transportation application. Compared to the conventional PM linear motor in compressor, the proposed modular model is designed with the same volume but a higher thrust force density and a further higher air pressure in air cylinder, which are competitive in the compressor industry. The proposed compact PM linear motors are constructed with tubular windings in both inner and outer stators, as well as the ring-type magnet in mover. Simulation results of motor characteristics are compared by three-dimensional finite element method (3D FEM). Finally, the prototypes of the proposed PM linear motors are manufactured and tested for the linear compressor application.

**Keywords:** dual-stator; linear compressor; permanent magnet motor; ring-type magnet



**Citation:** Zhao, F.; Jiang, Y.; Yang, K.; Zhang, C.; Lian, W.; Wang, G. Comparison Study on High Force Density Linear Motors for Compressor Application. *Energies* **2021**, *14*, 7417. https://doi.org/10.3390/en14217417

Academic Editor: Federico Barrero

Received: 9 September 2021
Accepted: 5 November 2021
Published: 8 November 2021



## 1. Introduction

In the application of electrified transportation, a rotary motor system generally has relative low efficiency and additional mechanical friction. In order to effectively eliminate the extra energy waste and save volume caused by the crank mechanism in the rotary motor system, the linear compressor motor is widely adopted due to its no crank mechanism, which can be directly oscillated by the inside drive motor and the helical coil springs [1–3]. As the relative high-performance linear motor, numerous PM linear motors have been developed for the linear compressor application, mainly aiming to improve the thrust force density, power, as well as efficiency [4–9].

Main topologies of the linear motors contain induction motors, switch reluctance motors, permanent magnet (PM) motors, and so on [3]. One classical production of the linear compressor is the high-grade LG linear compressor with a PM linear motor inside, which can be 20~30% more efficient than most efficient current crank driven compressors [4]. Basic configuration of this conventional PM linear motor in LG linear compressor [6,7] is shown in Figure 1a. Tubular winding has the advantages of compatible, easy manufacture and no end-winding effect. Unipolar magnet can be made as the ring-type, with the half height design compared to the outer-stator tooth. Furthermore, both of two stator cores are laminated based on the path of the magnetic flux, where outer stator cores are divided into eight segments for easy manufacture and inner stator core is listed in the circumferential pattern for less eddy current loss. Theoretically, the pieces of laminations are required to be installed tightly to obtain more useful magnetic flux.

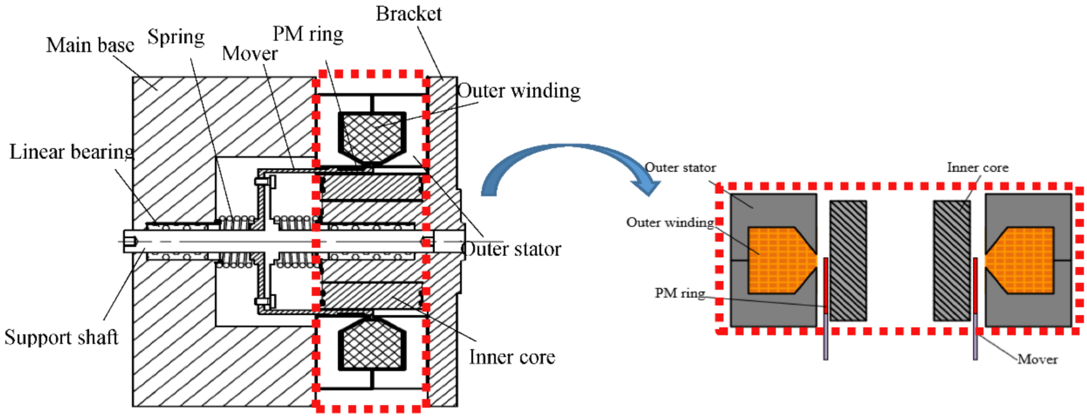


(**a**)

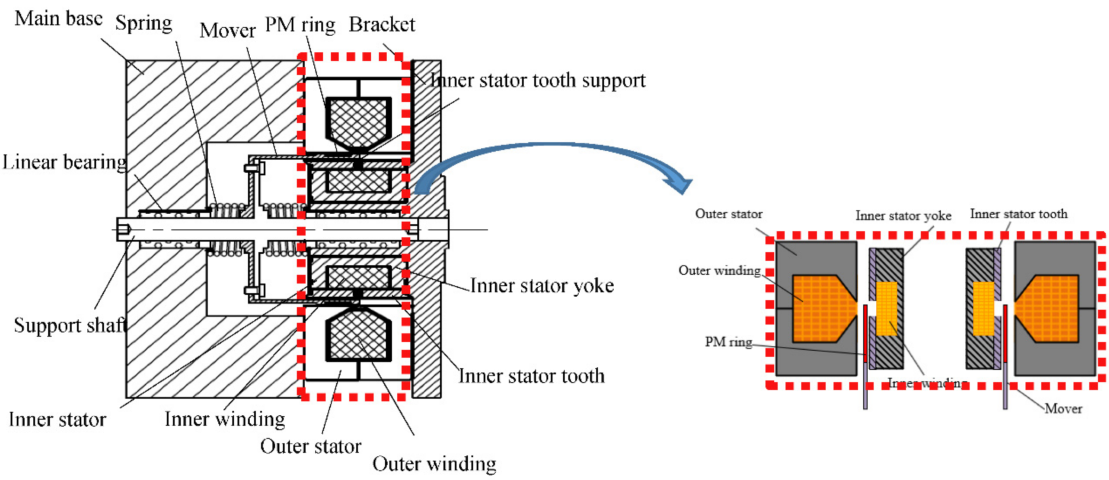


(**b**)

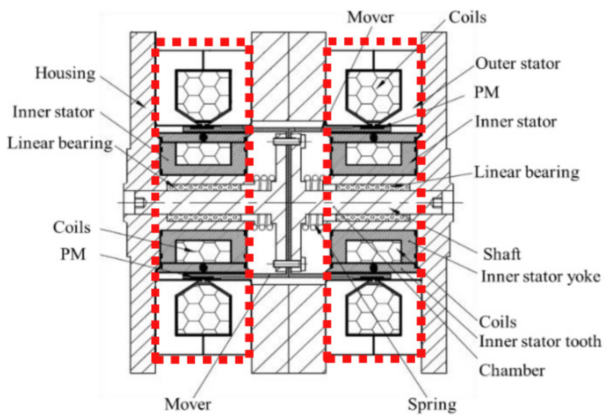


(**c**)

**Figure 1.** Discussed models: (**a**) Conventional model 1 without inner stator winding; (**b**) Proposed model 2 with inner stator winding; (**c**) Proposed model 3 as two modular model 2.

Based on the topology and dimension of the conventional PM linear motor, this paper presents new topology designs with practical application consideration. In [10], the dual-stator dual-winding design is introduced as one effective way to improve motor output performance with limited design dimensions. Therefore, two groups of stator tubular windings in both inner and outer stators are proposed, aiming to improve the motor thrust force density and air cylinder pressure with limited compressor installation space. Motor characteristics of the conventional and proposed motors in terms of flux linkage, back-EMF and thrust force, are evaluated by means of three-dimensional finite element method (3D FEM). Finally, the prototypes of the proposed motors are constructed and performance is experimentally validated for application on the electrified transportation linear compressor.

## 2. Design Approach of the Proposed Machine

### 2.1. Motor Topologies and Operating Principles

Figure 1 shows the motor topologies of the conventional model 1 and two proposed modular dual-stator PM linear motors as the proposed model 2 and model 3, respectively. Compared to the conventional PM motor in Figure 1a, the proposed models have an additional effective design of the inner stator tubular winding. In Figure 1b, the dual-stator dual-winding design is introduced as one effective way to improve motor output performance with limited design dimensions. As shown in Figure 2, two groups of stator tubular windings in both inner and outer stators are proposed in model 2, aiming to improve the motor thrust force density without increasing overall volume. In addition, model 3 utilizes the modular concept of the combination of two model 2 as Figure 1c to further increase the motor force density and fault tolerant ability, which contributes to the modular idea but not be taken into detail consideration in this research.

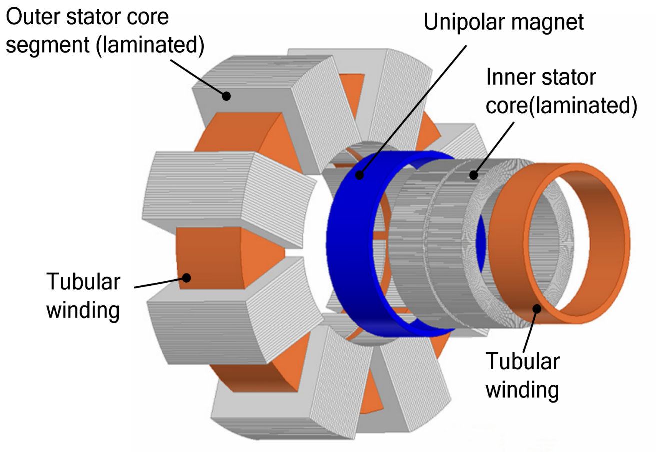


**Figure 2.** Configuration of the proposed model 2.

This kind of PM linear motor belongs to the magnet moving type of linear motor [11,12], where the mover support only needs to hold the unipolar magnet to achieve a light weight and the minimum inertia. In the mover, the rare-earth NdFeB magnet is preferred to be designed in ring-type to overcome the leakage flux between magnet pieces, where the magnet ring has good robustness but high cost for radial direction magnetization. To achieve the minimum iron loss and maximum motor efficiency, the stator core laminations are arranged in circumferential direction. In the conventional model 1, inner stator without winding is only used for magnetic flux modulation, so that the inner stator core laminations are arranged as the cooling fin structure. In the proposed models, the outer stator core laminations are designed as C-shape same as the conventional model for convenient comparison. The inner stator contains extra winding, thus its core laminations should be designed as two parts—yoke and tooth segments, which are manufactured separately for easy installation of winding. Both of the overall bracket and the tooth support are utilized to hold on the inner stator teeth during operation. Detailed design parameters of the conventional and proposed models are listed and compared in Table 1.

**Table 1.** Design parameters of electromagnetic parts in three motors.

| Items | Unit | Model 1 | Model 2 | Model 3 |
|---|---|---|---|---|
| Current density $J_c$ | A/mm$^2$ | 6~8 | 6~8 | 6~8 |
| Overall outer radius $R_o$ | mm | 82 | 82 | 82 |
| Inner stator outer radius $R_{io}$ | mm | 32 | 32 | 32 |
| Inner stator inner radius $R_{ii}$ | mm | 23.5 | 18 | 18 |
| Motor axial length $l$ | mm | 52 | 52 | 104 |
| Outer airgap length $g_o$ | mm | 1 | 1 | 1 |
| Inner airgap length $g_i$ | mm | 0.8 | 0.8 | 0.8 |
| Outer coil no. of turns $N_o$ | – | 800 | 800 | 800 |
| Inner coil no. of turns $N_i$ | – | 0 | 150 | 150 |
| PM thickness $g_m$ | mm | 3 | 3 | 3 |
| PM height $l_{pm}$ | mm | 25 | 25 | 50 |
| Magnet (NdFeB) | – | $B_r$ = 1.23 T, $H_c$ = −890 kA/m | | |

In the practical operation, the linear motor will be directly coupled to the compressor load and judged by the thrust force and pressure in air cylinder. The thrust force as the important output quality, is generated as the result of the interaction between the PM magnetic field and the stator winding current field. In addition, a couple of helical coil springs are selected as the resonant spring due to the low cost and compact structure, to contribute to start and control the mover oscillation. In addition, suction valve and suction flow path are placed on the piston to minimize flow resistance and suction heating loss. In the piston compressor, the capability of the air cylinder equals piston surface area multiples its diameter. Therefore, it takes more parameters design into consideration in the selection of the diameter and the stroke of piston.

### *2.2. Design Principle of the PM Linear Motors*

The proposed dual-stator dual-winding PM linear motor, with eight groups of C-shape core segments in the outer stator and two tubular windings, is designed following the conventional linear PM motor design principle [5,6]. Number of turns in the inner stator winding is limited by the out diameters of the bracket and inner stator core. Compact winding sleeve and ring-type magnet are adopted due to their easy installation and robustness [13].

Airgap electromagnetic field parameters are analyzed as expressed in (1) and (2). Assuming that the relative permeability of the permanent magnet is close to 1 and there is no magnetic motive force (MMF) drop in the core. Magnetic flux $\Phi_{in}$ flowing through inner stator core contains the flux components from the outer stator winding, PM and the extra inner stator winding, which is expressed as:

$$\Phi_{in} = k_\Phi \sum_{k=0}^{n} \int_{k\alpha}^{2\pi/p+k\alpha} B(x)dx = k_\Phi \int_{k\alpha}^{2\pi/p+k\alpha} (k_o B_O + k_g B_g + k_i B_i)dx \quad (1)$$

where $B$ is flux density, $x$ is the circumference distance, $\alpha$ is the tooth span, $p$ is the outer stator core segment number, $n$ is component number. $K_o B_o$, $k_g B_g$ and $k_i B_i$ are the flux from outer stator, airgap and inner stator, respectively. The magnetic force $F_{mag}$ can be expressed as:

$$F_{mag} = \frac{\partial W_{\mathrm{m}}}{\partial x} = k_e \int B(x)F(x)dx \tag{2}$$

where the quantity $W_m$ is the field energy product, $k_e$ is the motor energy coefficient, $F$ is the MMF in airgap, and $x$ is along motor mover axis.

## 3. Characteristics Analysis and Comparison

Simulation models of the conventional and proposed PM linear motors are built only considering the effective electromagnetic structures. Three-dimensional FEM is considered as an efficient and accurate method to evaluate the magnetic field features for the 3D electromagnetic problem. Only considering the electromagnetic structure, model 3 is a combination of two model 2, thus only motor characteristics of model 1 and model 2 are compared in this section.

Figure 3 presents the flux density vector distributions in two models without current excitation to verify the original no-load flux loop design, where the mover is located at the starting point. The flux density distributions under the rated current excitation are shown in Figure 4, which are used to verify the design reasonability without core saturation in the full load condition. The ending position of mover is selected, because the core flux density achieves maximum at this moment. In addition, the flux density comparison demonstrates a higher and well distributed flux density in the inner stator of the proposed model 2 with the extra armature excitation in the inner stator.

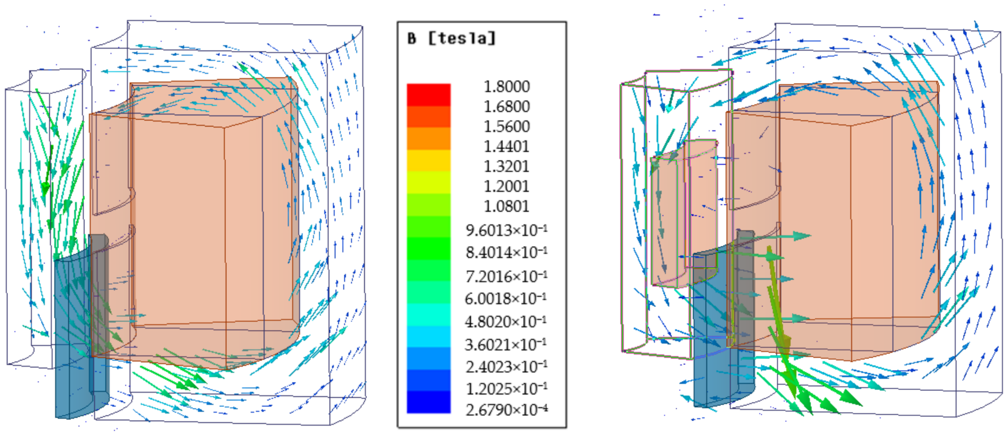


**Figure 3.** No-load flux density vector distributions: (**a**) Conventional model 1; (**b**) Proposed model 2.

Moreover, Figure 5 shows the comparison waveforms of the winding flux, back-EMF, and thrust force of the two models. In the absence of current excitation, that is, when the motor is under no load, the two models are simulated to obtain the waveforms of flux linkage and the back-EMF. In order to evaluate the machine performance in different conditions, the thrust force waveforms is obtained under constant DC current excitation in Figure 5c, where sinusoidal current excitation is used in Figure 5d with the amplitude value same with DC current. In order to illustrate the basic characteristics of the mover clearly, simulations are operated with the same constant speed. Through formula (3), the motor running speed can be calculated is 2.8 m/s.

$$v = 2\,f\,\tau \tag{3}$$

where, the quantity $f$ is oscillation frequency, $\tau$ is the motor pole pitch, $v$ is the velocity of mover.

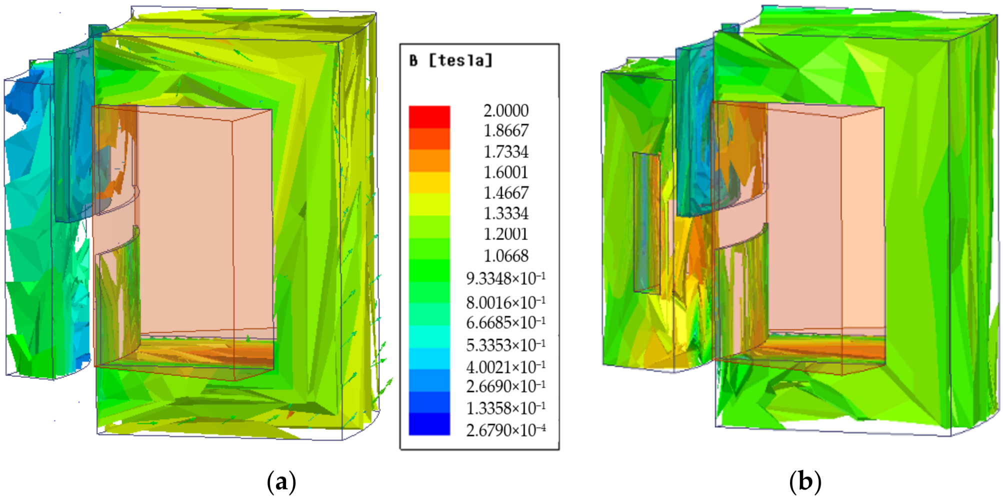


**Figure 4.** Loaded flux density distributions: (**a**) Conventional model 1; (**b**) Proposed model 2.

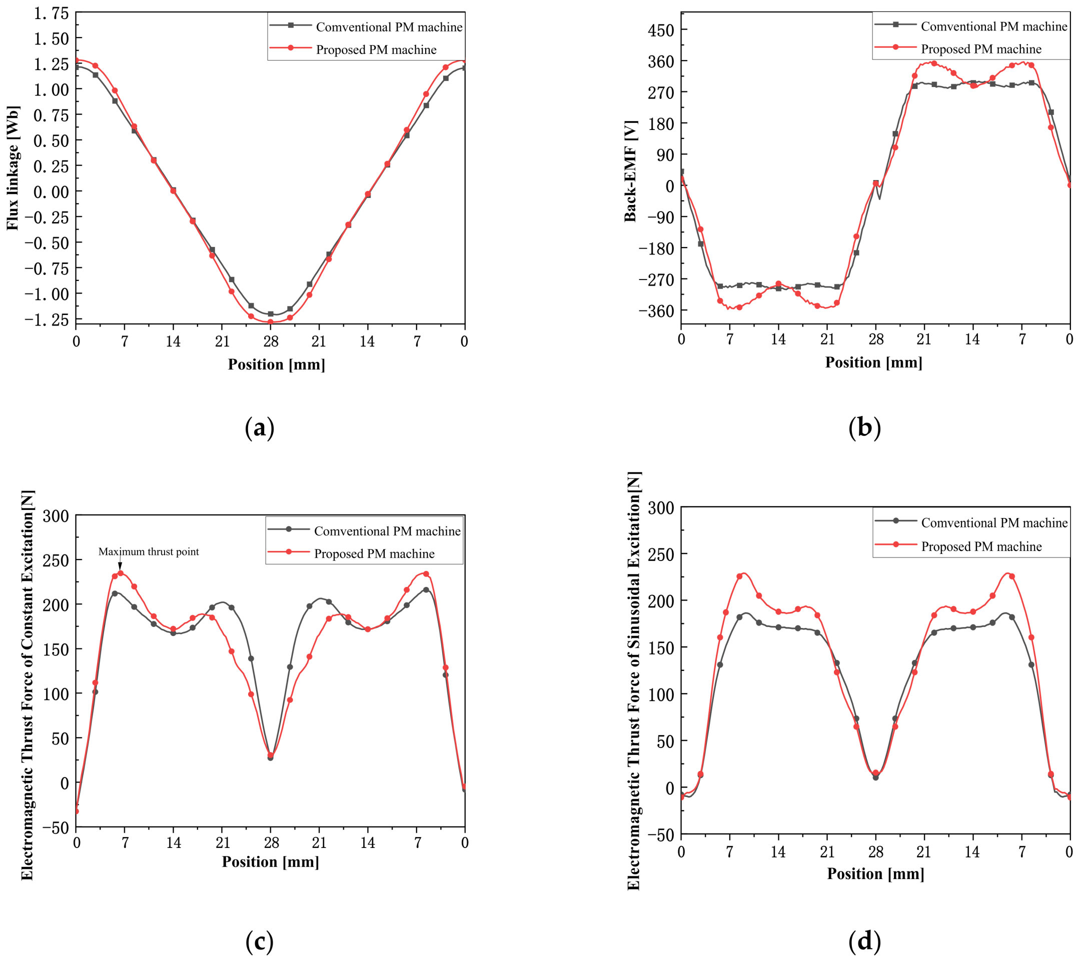


**Figure 5.** Characteristics comparison of the conventional model 1 and the proposed model 2: (**a**) Flux linkage waveforms; (**b**) back-EMF waveforms; (**c**) Electromagnetic thrust force under constant DC current excitation; (**d**) Electromagnetic thrust force excited by sinusoidal current.

It can be clearly seen from Table 2 that, the flux linkage, back-EMF, and the maximum thrust under rated load of the proposed model 2 have obvious improvement compared with model 1, which is mainly caused by additional winding setting in the inner stator.

**Table 2.** Comparison of simulation parameters of two models.

| Items | Unit | Model 1 | Model 2 | Percentage Change |
|---|---|---|---|---|
| Maximum flux linkage | Wb | 1.21 | 1.28 | +5.78% |
| Maximum back-EMF | V | 299.84 | 350.08 | +16.76% |
| Maximum thrust force | N | 215.95 | 249.23 | +15.41% |
| Output power $P$ | W | 468.33 | 497.06 | +6.13% |
| Copper loss $P$cu | W | 70.05 | 76.15 | +8.72% |
| Motor efficiency $\eta$ | – | 85.81% | 86.57% | +0.77% |

## 4. Prototype and Experimental Discussion

Figure 6a shows the photos of the motor inner stator yoke and tooth segments separately, where the tooth segment will be assembled to the yoke segment after the inner stator tubular winding wound. Moreover, a non-magnetic material mass with 3 mm length is used to support the airgap between the inner stator teeth shoes. This kind of new manufacture technique in circumferential direction core lamination is firstly used for easy tubular winding layout. Two modular prototypes of the proposed model 2 and model 3 are manufactured as in Figure 7a,b, respectively.

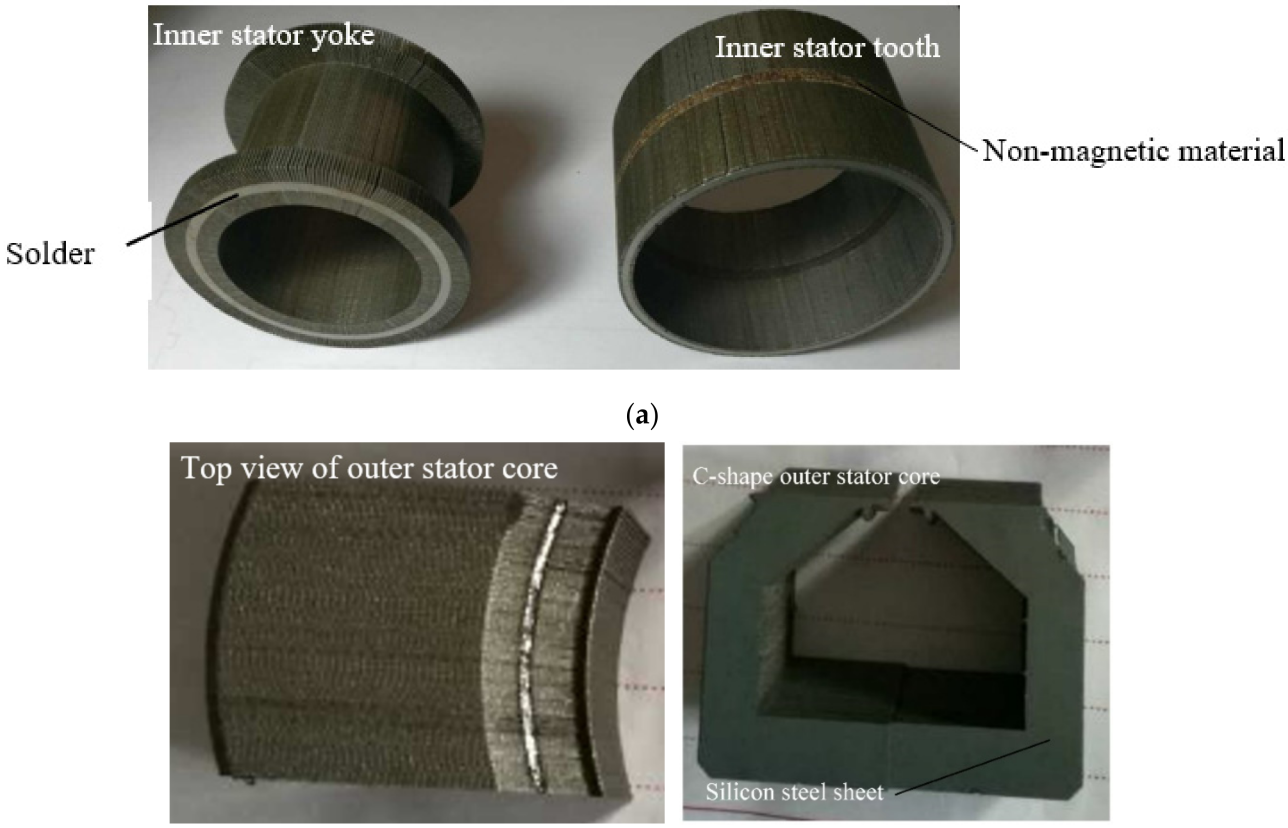


(**a**)

(**b**)

**Figure 6.** Stator core laminations of the proposed models: (**a**) Inner stator yoke tooth; (**b**) Outer stator core.

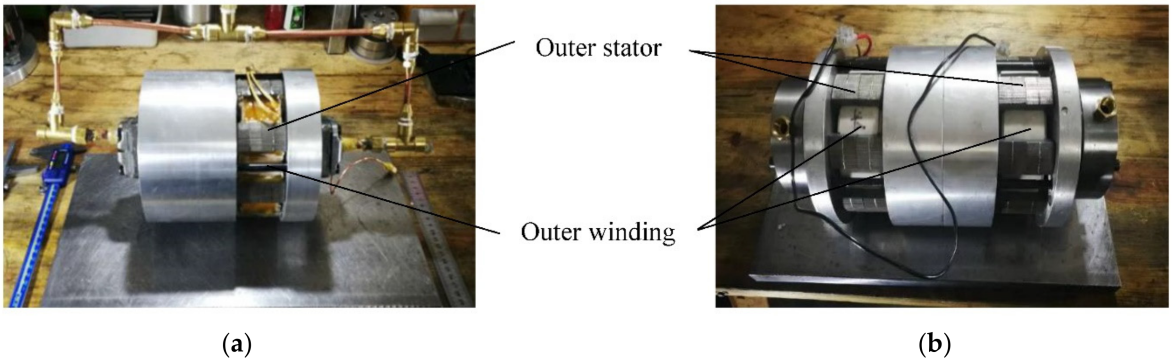


**Figure 7.** Prototypes of the proposed model 2 and model 3: (**a**) Prototypes of the proposed model 2; (**b**) Prototypes of the proposed model 3.

Figure 8 presents the test results of the prototype of model 2 on the phase current and maximum stroke versus frequency under a voltage limitation of 150 V. Since model 3 can be considered as two modular model 2, its prototype is also tested in same frequency and phase current. A normal control board of linear motor is used to test the basic motor feature limited by a relative low frequency of 15 Hz. In the low frequency operation range, the stroke distance increases with higher frequency. A maximum value will occur when the excitation frequency equals to the resonant frequency of the motor, where the system efficiency will achieve maximum too. Moreover, the phase current decreases with higher frequency in low frequency range, there will also be a relative low current low input power point to achieve maximum efficiency. In addition, the higher voltage supply will result in larger phase current and larger stroke distance for different linear compressors operation.

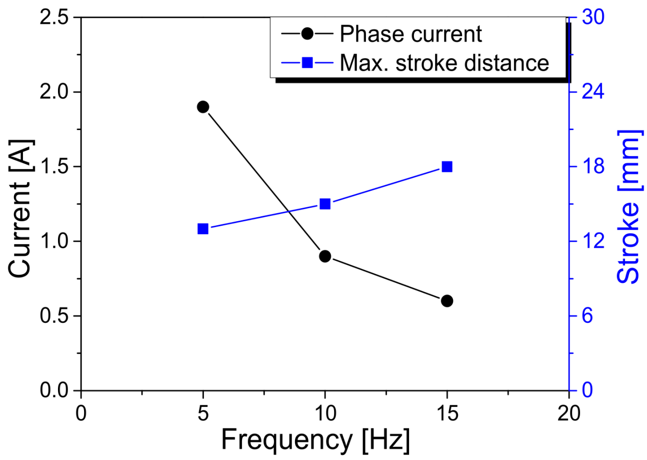


**Figure 8.** Test results of the prototype of model 2 in low frequency drive.

Table 3 illustrates basic experimental results compared to the original designed results of model 2 to verify the prototype suitable for the linear compressor application. Due to the control board limitation, experimental results under a relative low voltage and low frequency range were tested as in Figure 8. The motor characteristics of maximum stroke distance and maximum air pressure in the air cylinder are illustrated to show the basic characteristics with low frequency operation.

**Table 3.** Prototype experimental results and comparison.

| Items | Unit | Designed Model 2 | Prototype of Model 2 | Prototype of Model 3 |
|---|---|---|---|---|
| Max. stroke distance *d* | mm | 22 | >18 | >20 |
| Mover mass *m* | kg | 0.42 | 0.55 | 1.41 |
| Max. air pressure in air cylinder *P* | kg | >16 | 20 | 42 |

## 5. Conclusions

This paper proposes a type of permanent magnet linear motors with two tubular windings in both inner and outer stators. Compared with the conventional permanent magnet linear motor, the motor has higher thrust density, higher output power, high efficiency, and achieves the effect of energy saving, which is suitable for compressors. The proposed model 2 has the same outer stator, the same outer stator winding volume, and the same air gap length with the conventional model 1. Model 3 is designed as a dual module of model 2 to pursue higher thrust. The characteristics of these motors were evaluated by 3D-FEM to verify the expected advantages of the additional inner tubular winding design. Finally, the experimental results under lower voltage and lower frequency range were tested, and its basic operating characteristics were explained.

**Author Contributions:** Conceptualization, writing-original draft F.Z.; data curation, Y.J.; software, K.Y.; investigation, C.Z.; validation, W.L.; resources, G.W. All authors have read and agreed to the published version of the manuscript.

**Funding:** This research received no external funding.

**Institutional Review Board Statement:** Not applicable.

**Informed Consent Statement:** Not applicable.

**Data Availability Statement:** Not applicable.

**Acknowledgments:** This work was supported in part by Guangdong Basic and Applied Basic Research Foundation 2021A1515010754, and the Basic Research Plan in Shenzhen City (Grant No. JCYJ20180507181539943 and JCYJ20190806142618203).

**Conflicts of Interest:** The authors declare no conflict of interest.

## References

1. Utsuno, M.; Takai, M.; Yaegashi, T.; Mizuno, T.; Yamamoto, H.; Shibuya, K.; Yamada, H. Efficiency characteristics of a linear oscillatory actuator under simulated compressor load. In Proceedings of the 2001 Linear Drives and Industry Applications (LDIA'2001), Nagano, Japan, 17–19 October 2001; pp. 264–267.
2. Chun, T.; Ahn, J.; Yoo, J.; Lee, C. Analysis and control for linear compressor system driven by PWM inverter. In Proceedings of the 30th Annual Conference of the IEEE Industrial Electronics Society, Busan, Korea, 2–6 November 2004; pp. 263–267.
3. Wang, J.; Howe, D.; Lin, Z. Comparative studies on linear motor topologies for reciprocating vapour compressors. In Proceedings of the International Electrical Machines and Drives Conference (IEMDC2007), Antalya, Turkey, 3–5 May 2007; pp. 364–369.
4. Lee, H.; Song, G.; Park, J.; Hong, E.; Jung, W.; Park, K. Development of the linear compressor for a household refrigerator. In Proceedings of the International Compressor Engineering Conference, West Lafayette, IN, USA, 25–28 July 2000; Purdue e-Pubs: West Lafayette, IN, USA, 2000.
5. Chen, X.; Jiang, H.; Li, Z.; Liang, K. Modelling and measurement of a moving magnet linear motor for linear compressor. *Energies* **2020**, *13*, 4030. [CrossRef]
6. Xia, Y.; Lu, Q.; Ye, Y.; Kang, R. Analysis and modeling of a new type of dual-stator linear oscillation motor. *Trans. Chin. Soc. Electr. Eng.* **2007**, *12*, 29–33.
7. Hur, K.; Lee, H. Linear Compressor. U.S. Patent 6398523B1, 4 June 2002.
8. Ibrahim, T.; Wang, J.; Howe, D. Analysis and experimental verification of a single-phase, quasi-halbach magnetized tubular permanent magnet motor with non-ferromagnetic support tube. *IEEE Trans. Magn.* **2008**, *44*, 4361–4364. [CrossRef]
9. Wang, J.; Howe, D.; Lin, Z. Design optimization of short-stroke single-phase tubular permanent-magnet motor for refrigeration applications. *IEEE Trans. Ind. Electron.* **2010**, *57*, 327–334. [CrossRef]
10. Kwon, Y.; Kim, W. Detent-force minimization of double-sided interior permanent-magnet flat linear brushless motor. *IEEE Trans. Magn.* **2016**, *52*, 8201609. [CrossRef]

11. Kim, T.; Lee, H.; Kim, Y.; Lee, J.; Boldea, I. Development of a flux concentration-type linear oscillatory actuator. *IEEE Trans. Magn.* **2004**, *40*, 2092–2094. [CrossRef]
12. Clark, R.; Jewell, G.; Howe, D. Dynamic modeling of tubular moving-magnet linear actuators. *J. Appl. Phys.* **2003**, *93*, 8787–8789. [CrossRef]
13. Xu, J.; Zhao, W.; Wang, X.; Wang, X.; Wang, F. Design and analysis of a novel dual-stator tubular linear machine with split teeth structure. In Proceedings of the 13th International Symposium on Linear Drives for Industry Applications (LDIA), Wuhan, China, 1–3 July 2021; pp. 1–5.